

## The Analysis of a Modified Version of the SEPIC Dc-Dc Converter Used as Pre-Regulator Operating in Discontinuous Conduction Mode



Vemula Vinod Kumar  
M.Tech,

Arjun College of Technology and Sciences.



Rosaiah Mudigondla, M.Tech(PEED)  
Assistant Professor,

Arjun College of Technology and Sciences.

### ABSTRACT:

The hypothetical and trial examination of a adjusted form of the SEPIC DC-DC converter utilized as pre-controller working as a part of irregular conduction mode (DCM) is exhibited in this paper. The proposed converter introduces a low info current swell working in DCM and the switch voltage is lower than the yield voltage. The switch voltage lessening builds the converter unwavering quality and a low deplete to-source on-resistance (RDSon) MOSFET can be utilized relying upon the converter determination. Also, an advanced control strategy is connected to the proposed converter to decrease the third consonant information current contortion resultant of the operation in DCM. At last, a 100W model was produced working with productivity equivalent to 95.6%.

### Index Terms:

AC-DC power conversion, Rectifiers, Digital control.

### I. INTRODUCTION:

The standard answer for the execution of a powerful variable (HPF) pre-controller for a low yield power application ( $P_o < 200W$ ) is to utilize a support converter working in irregular conduction mode (DCM) [1]-[2]. This is a basic and practical arrangement on the grounds that the outline of the rectifier in DCM permits the converter to work as a voltage devotee, where the info current normally takes after the

Information voltage profile without the utilization of a present control circle. The operation in DCM decreases the substitution misfortunes since the switch turn-on happens with zero-current-exchanging (ZCS) and the yield diode does not present converse recuperation current. This arrangement is restricted for low power applications because of an expanded converter conduction misfortunes working in DCM. Since the info inductor of the help converter works in DCM, a high recurrence channel made by an inductor  $L_f$  and capacitor  $C_f$  should be utilized as a part of the pre-regulator input in order to reduce the input current ripple, as presented in Fig. 1.

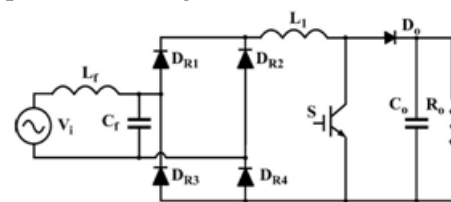


Fig. 1. Classical boost pre-regulator operating in DCM.

Be that as it may, an issue exhibited by the support pre-controller working in DCM is the information current contortion, showing a third consonant part. The voltage connected over the information inductor amid its demagnetization is equivalent to the yield voltage less the info voltage, consequently, the present bending increments when the distinction between the yield voltage and the pinnacle info voltage is decreased. In this manner, the yield voltage can be expanded,

lessening the third symphonious information current twisting and enhancing the force component. Likewise a variable obligation cycle control can be utilized as a part of request to lessen the info current mutilation as displayed in area V. The support converter can work with unitary force consider freely of the contrast between the yield and info voltage working at the limit of the DCM and constant conduction mode (CCM) with a variable exchanging recurrence regulation. The traditional SEPIC converter, appeared in Fig. 2, shows a stage up/venture down static increase and for the most part is utilized as a HPF pre-controller in applications where the yield voltage must be lower than the pinnacle of the AC information voltage [3]-[4]. The usage of the pre-controller utilizing the traditional SEPIC converter as a part of DCM presents two extra operation attributes. Firstly, the converter works as a voltage devotee when planned in DCM with a low esteem for the inductor  $L_2$  and utilizing a high esteem for the inductor  $L_1$ , yet the info current displays a low current swell pretty much as a support rectifier working in CCM with current control circle. Therefore, the  $L_f$ - $C_f$  channel utilized as a part of the support converter info working in DCM is a bit much utilizing the SEPIC converter working as a part of DCM.

Thusly, the amount of parts for both converters working in DCM is proportionate. Nevertheless, in a sensible application, an electromagnetic impedance (EMI) divert is key as in any rectifier topology. The second vital trademark utilizing the SEPIC converter as a part of DCM is that the info current takes after the information voltage waveform without information current mutilation. The third consonant mutilation is not introduced on the grounds that the inductor  $L_2$  is demagnetized with the yield voltage. All things considered, the support converter is the favored topology utilized for the pre-controller application where the yield voltage must be higher than the pinnacle of the information voltage, given that the switch voltage of the SEPIC converter is equivalent to the entirety of the info and yield voltages.

The SEPIC converter can be effectively utilized as a part of uses where the yield voltage is lower than the info voltage. A few high-productivity bridgeless arrangements utilizing the SEPIC and CUK converters are exhibited in [5]-[10].

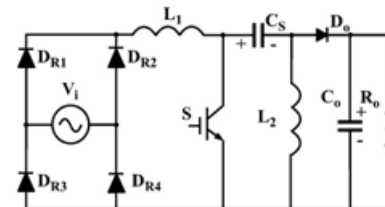


**Fig. 2. Classical SEPIC pre-regulator operating in DCM.**

The adjusted SEPIC converter utilized as pre-controller working as a part of DCM is appeared in Fig.3. An altered SEPIC DC-DC converter was proposed in [11] with the incorporation of an extra diode ( $D_M$ ) and capacitor ( $C_M$ ) at the established SEPIC converter, changing a few qualities, for example, the operation with a switch voltage lower than the yield voltage. Be that as it may, just the operation as DC-DC converter in CCM was broke down in [11]. This converter was additionally utilized as a part of [12] as a pre-controller working in CCM displaying a few favorable circumstances when contrasted and the traditional support pre-controller working in CCM for all inclusive line info application (90Vrms - 260Vrms).

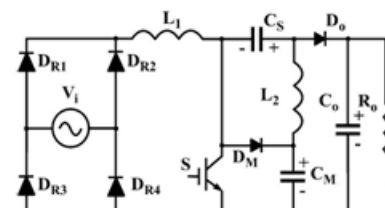


**Fig. 3. Modified SEPIC pre-regulator operating in DCM.**

Regardless, the hypothetical and trial investigations of the changed SEPIC converter working in DCM as a DC-DC converter and pre-controller were not introduced yet, which is center of this paper. The proposed topology shows the same impediments of the traditional support converter when contrasted and the established SEPIC converter since its operation is

exclusively conceivable as a non-secluded converter with venture up static addition. Uniquely in contrast to the established SEPIC converter, a helper inrush impediment circuit must be incorporated for the rectifier start-up. Additionally, the force element is lower than the traditional SEPIC converter because of the third symphonious part in the info current. In any case, the force element and the info current contortion of the altered SEPIC converter can be essentially enhanced applying a straightforward open circle activity utilizing the information and yield voltage data. The utilization of the help and adjusted SEPIC rectifiers are just conceivable in applications with a yield voltage higher than the pinnacle of the info voltage and proposals rectifiers are more appropriated than the SEPIC converter with the same specification, since the SEPIC converter displays a high switch voltage. The lowest switch voltage level is presented by the modified SEPIC topology. The adjusted SEPIC converter works as a voltage supporter and the information current shows low current swell, for example, an established SEPIC converter, planning the converter in DCM and utilizing a low esteem for the inductor L2 and a high esteem for the inductor L1. The fundamental converter attributes and investigations are introduced in the accompanying, with the hypothetical operation improvement of the proposed converter.

## II. THEORETICAL ANALYSIS:

The circuit of the pre-controller utilizing the adjusted SEPIC converter working in DCM is introduced in Fig. 3. The principle contrast from the pre-controller displayed in [12] is the operation mode and the control framework that is formed by just a voltage control circle due to the DCM operation. Additionally, the non-dissipative current snubbed utilized as a part of [12] is a bit much on the grounds that the converse recuperation current of the diodes and the turn-on exchanging misfortunes working in CCM are diminished with the DCM operation.

The altered SEPIC DC-DC converter working in DCM presents three operation stages. The hypothetical investigation is at first created considering the operation as a DC - DC converter at unflinching state

and all circuit parts are viewed as perfect. The voltages over all capacitors are viewed as steady amid an exchanging period, as a perfect voltage source. The DCM operation happens when there is the third operation stage, where the force switch is killed and the streams in all diodes of the circuit are invalid. Consequently, the DCM operation happens when Do and DM diodes are obstructed before the switch turn-on. The investigation and configuration method is likewise created for the operation as a pre-controller with a diode span at info and an AC information voltage, taking into account the study as DC-DC converter. The circuit presents two inductors, in this manner, diverse inductor values mix can be embraced for the DCM operation. So as to lessen the info current swell of the pre-controller, a relative high esteem for the inductor L1 is considered. A relative low estimation of the inductor L2 is utilized for the converter operation as a part of DCM as a voltage devotee, where the information current takes after the info voltage waveform. Subsequently, the pre-controller information current takes after the information voltage waveform with low current swell, without info channel and without current control circle. An important equation for the operation analysis of the converter is presented in (1). Considering the operation at steady state, the average voltage across the inductors L<sub>1</sub> and L<sub>2</sub> are null and the sum of the input voltage V<sub>i</sub> and capacitor C<sub>S</sub> voltage is equal to the capacitor C<sub>M</sub> voltage. The operation stages in DCM are presented as follows:

$$V_{CM} = V_i + V_{CS} \quad (1)$$

1) First Initially Stage [t<sub>0</sub> - t<sub>1</sub>] (Fig. 4) – During the conduction of the power switch S, the info inductor stores vitality with the information voltage connected crosswise over L<sub>1</sub> (V<sub>L1</sub>). The voltage connected crosswise over L<sub>2</sub> (V<sub>L2</sub>) is equivalent to the voltage of capacitor C<sub>M</sub> short the voltage of capacitor C<sub>S</sub>.

As displayed in (1), this voltage distinction is equivalent to the information voltage. Subsequently, inductors L<sub>1</sub> and L<sub>2</sub> store vitality in this operation stage and the same voltage is connected over these

inductors. The streams through inductors  $L_1$  and  $L_2$  increment taking after (3) and (4) separately, yet since  $L_2$  is lower than  $L_1$ , the present variety in  $L_2$  is higher than in  $L_1$ , as exhibited in the hypothetical waveforms appeared in Fig.7. The diodes  $D_M$  and  $D_o$  are obstructed amid this operation stage..

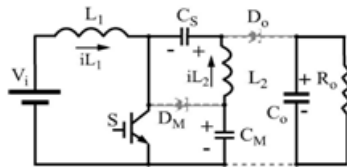


**Fig. 4. First operation stage.**

2) *Second Stage* [ $t_1 - t_2$ ] (Fig. 5) – At the instant  $t_1$ , switch  $S$  is turned-off and the energy stored in the input inductor  $L_1$  is transferred to the output through the  $C_S$  capacitor and output diode  $D_o$ . There is also energy transference to  $C_M$  capacitor through diode  $D_M$  and the maximum switch voltage is equal to the  $C_M$  capacitor voltage. The energy stored in inductor  $L_2$  is also transferred to the output and capacitor  $C_S$  through diodes  $D_o$  and  $D_M$ . The voltage applied across  $L_1$  is equal to  $C_M$  capacitor voltage minus the input voltage and this difference is equal to the  $C_S$  capacitor voltage as calculated by (1) . The voltage across the inductor  $L_2$  is equal to the negative capacitor  $C_S$  voltage. Thus, the voltage applied across the inductor  $L_1$  and  $L_2$  are equal to the negative capacitor  $C_S$  voltage during this operation stage and the inductor current variation is calculated by (6) and (7) respectively. As presented in Fig. 7, the time interval ( $t_2-t_1$ ) of the second operation stage is defined as  $t_d$  and is equal to the transference period of the energy stored in inductors  $L_1$  and  $L_2$  through diodes  $D_o$  and  $D_M$ . When  $L_2$  current value becomes equal to  $L_1$  current value with the same direction, the currents at diodes  $D_o$  and  $D_M$  becomes null, finishing this operation stage. Therefore,  $t_d$  is the conduction time of diodes  $D_M$  and  $D_o$ , when the energy stored in the inductors  $L_1$  and  $L_2$  is transferred.

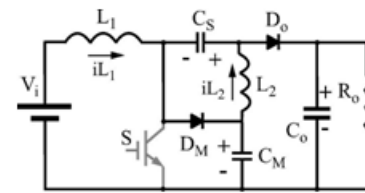


**Fig. 5. Second operation stage.**

3) *Third Stage* [ $t_3 - t_4$ ] (Fig. 6) – When diodes  $D_o$  and  $D_M$  are blocked at the instant  $t_3$ , the voltage applied across the inductors  $L_1$  and  $L_2$  are null, maintaining the inductors currents constant as presented in (9) and (10). The currents through the inductors  $L_1$  and  $L_2$  present the same value, operating as a freewheeling stage. This operation stage is finished when the power switch is turned-on at the instant  $t_4$ , returning to the first operation stage.

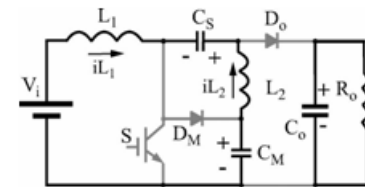


**Fig. 6. Third operation stage.**

The main theoretical waveforms are presented in Fig. 7. The switch turn-on occurs with ZCS such as a classical DC-DC converter operating in DCM and the diodes do not present reverse recovery current. The maximum switch voltage is equal to the capacitor  $C_M$  voltage and this voltage is lower than the output voltage. The  $L_1$  inductor average current is equal to the input current and the  $L_2$  inductor average current is equal to the output current. The average current in the capacitors  $C_S$  and  $C_M$  are null at steady state, thus, the average current of diodes  $D_M$  and  $D_o$  are equal to the output current.

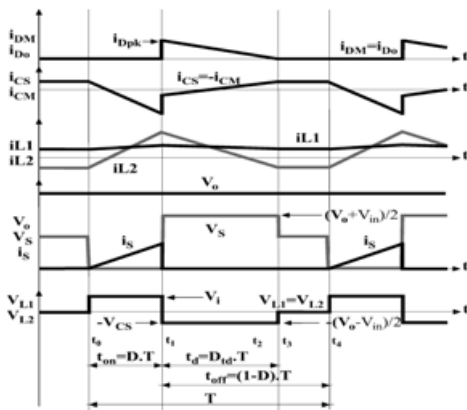


Fig. 7. Main theoretical waveforms.

A. Converter static gain and the capacitors  $C_s$  and

VI. OUTPUT VOLTAGE CONTROL SYSTEM

A. Control-to-output transfer function ( $v_o(s)/d(s)$ )

A dynamic model of switching converter is required for feedback control loop. However, the power converters are described by a set of the nonlinear differential equations. Usually is easier to analyze a small-signals model that is linearized related to the quiescent operation point in order to obtain a linear model, as presented in [15]. The small signal equivalent circuit of buck, boost and buck-boost converters presents a capacitor and inductor, operating in DCM. The transfer functions have two poles. One pole is due to the output capacitor, at low frequency, and other pole, in much higher frequency due to the inductor. For this reason, an approximate way to determine the low frequency small-signal transfer function of the basics converters is to let the inductance tend to zero [15]. Also, the capacitor  $C_M$  and  $C_S$  are very small in the modified SEPIC converter, where  $C_o \gg C_M$  and  $C_o \gg C_S$ . Therefore, they can be neglected to obtain control-to-output transfer function for low frequency. In this case, the high frequency capacitors dynamics can be ignored. The modified SEPIC without  $C_M$ ,  $C_S$  and  $L_1$  is shown in Fig. 13(a) and the equivalent circuit is shown in Fig. 13(b). The remaining model is solved for the low-frequency converter dynamics.

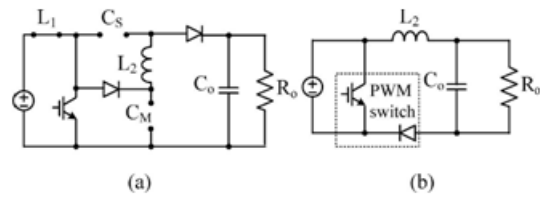


Fig. 13. Simplified circuit model of modified SEPIC DC-DC: (a) with neglected components, (b) equivalent circuit.

To perform this analysis, the model of the PWM switch in DCM proposed in [16] is used considering the equivalent circuit presented in Fig. 13(b). The equivalent circuit of an average model and small-signal model of PWM switch in DCM is shown in Fig 14. Transfer function is obtained considering a resistive load. The model of the PWM switch in DCM is replaced in the modified SEPIC converter and the input voltage is shortened. Figure 15 shows the equivalent circuits.

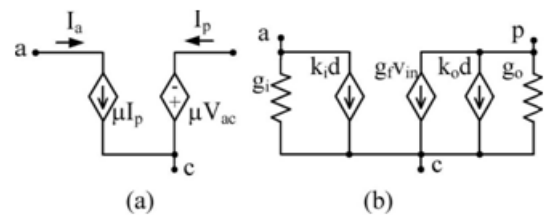


Fig. 14. Model of PWM switch in DCM: (a) Average model (b) Small-signal model.

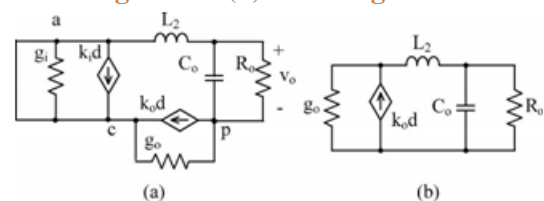
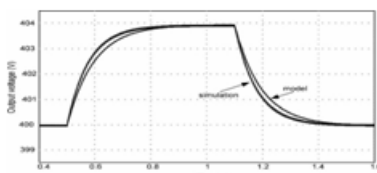


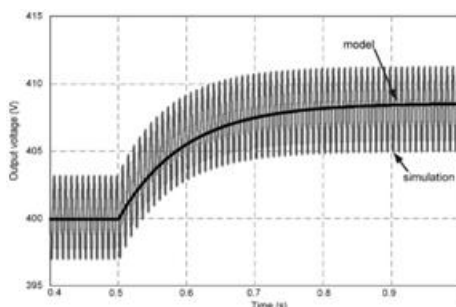
Fig. 15. Small-signal equivalent circuit for control-to-output transfer function of modified SEPIC: (a) complete circuit (b) simplified circuit.

Figure 16 shows the dynamic behavior of the output voltage waveform under duty-cycle disturbances considering the operation as a DC-DC converter. At 0.5 s, a 1% step is applied in the duty-cycle. At 1.1s, the duty-cycle returns to its nominal value. The results show good resemblance between the proposed model and the simulation of the converter power circuit.

The dynamic response of the proposed converter operating in DCM is an over damped second order system with a step response similar to a first order system. The modified SEPIC rectifier presents an oscillating input voltage with double line frequency. On the other hand, a large output capacitor is used to minimize the output voltage ripple. Thus, output voltage does not change significantly in a half-line period and a simplified model can be considered without the input ripple. The simulation result of the modified SEPIC operating as a rectifier and the prediction of the small signal model for a step change in the duty-cycle are shown in Fig. 17. It can be observed that this model gives good results at low frequencies. It cannot accurately predict high frequency dynamics because  $C_M$ ,  $C_S$  and  $L_1$  are neglected. However, the output voltage feedback loop in the conventional rectifier control system must have a low- bandwidth in order to avoid distortions in the input current waveform. The controller should have sufficiently small loop gain at the even harmonics of the AC line frequency. Therefore, low-frequency small-signal transfer function is appropriate for the control of the modified SEPIC rectifier.



**Fig. 16. Comparison of the transient responses of output voltage for a 1% disturbance in the duty-cycle for the modified SEPIC operating as a DC-DC converter in DCM**



**Fig. 17. Comparison of the transient responses of output voltage for a 2% disturbance in the duty-**

**cycle for the modified SEPIC operating as a rectifier in DCM.**

### B. Control System

The pre-regulator operation in DCM allows obtaining high power factor without a current control loop and only a voltage control loop is necessary [14]. The output voltage control algorithm used in the proposed converter is based on the classical PI controller. The design procedure can be simplified using a design procedure similar to the classical boost converter. Also, the 120 Hz ripple of the pre-regulator output voltage must be rejected by the voltage control loop in order to maintain the high power factor operation. Therefore, the voltage control loop presents a very slow dynamic response such as any classical pre-regulators. The block diagram of the digital control implementation is presented in Fig. 18, including the third harmonic reduction technique. Only the output and input voltages are necessary to control the pre-regulator. The control algorithm was developed using a digital signal processor TMS320F2812, operating with sampling rate equal to 30 kHz. The sampled output voltage signal is compared to an output voltage reference and the error is applied to a PI voltage controller. Simultaneously, the sampled rectified input voltage and the output voltage reference are applied to (63) in order to calculate the duty -cycle variation for the third harmonic reduction. The result of the PI output voltage controller and the result of the third harmonic reduction are multiplied obtaining the pre-regulator duty-cycle and generating the PWM signal that controls the switch  $S$ .

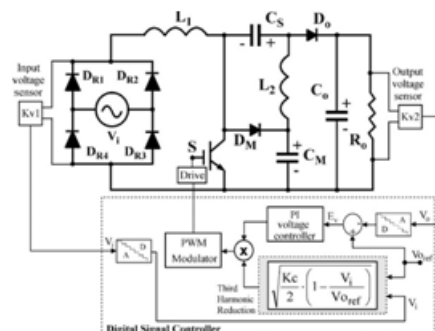


**Fig. 18. Block diagram of the pre-regulator control system.**

**VII. EXPERIMENTAL RESULTS:**

The proposed pre-regulator was implemented as presented in Fig.18 using the specifications presented in Table I and the components used are shown in Table IV. The pre-regulator performance is compared with and without the implementation of the third harmonic reduction technique. The waveforms were obtained with nominal output power and input voltage equal to 127 V<sub>rms</sub> and 220 V<sub>rms</sub>. The pre-regulator input current and voltage waveforms, operating with V<sub>i</sub> = 127 V<sub>rms</sub> and without the third harmonic distortion reduction technique are presented in Fig. 19.

**TABLE IV**

**Pre-regulator components**

Parameter	Pre-regulator with modified SEPIC converter
Inductor L <sub>1</sub>	L <sub>1</sub> = 6.8 mH ESR=692 mΩ
Inductor L <sub>2</sub>	L <sub>2</sub> = 540 μH ESR=98 mΩ
Capacitor C <sub>S</sub>	C <sub>S</sub> =220 nF ESR=10 mΩ
Capacitor C <sub>M</sub>	C <sub>M</sub> =220 nF ESR=10 mΩ
Output capacitor C <sub>o</sub>	C <sub>o</sub> =120 μF ESR=390 mΩ
Diodes D <sub>M</sub> -D <sub>o</sub>	D <sub>M</sub> =D <sub>o</sub> =UF5408 V <sub>F</sub> =1.7 V
Power switch S	S=FQA28N50 V <sub>DSS</sub> =500 V R <sub>Dson</sub> =0.16 Ω (25°C)

The total input current harmonic distortion is equal to 13% without the application of the third harmonic reduction technique and the pre-regulator power factor is equal to 0.993. The total input voltage harmonic distortion is equal to 3.1%.

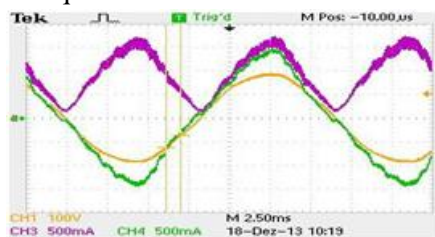


**Fig. 19. Input voltage and current operating with V<sub>i</sub>=127 V<sub>rms</sub> and without the third harmonic reduction technique (CH1 - Input voltage - 100 V/div, CH3 - L<sub>1</sub> current - 0.5 A/div, CH4 - Input current - 0.5 A/div).**

The pre-controller information current and voltage waveforms, working with V<sub>i</sub> = 127 V<sub>rms</sub> and with the third symphonious twisting decrease strategy are exhibited in Fig. 20. The aggregate information current symphonious contortion is decreased to 5.3% with the utilization of the third consonant lessening system and the pre-controller power variable is expanded to 0.999. Considering that the aggregate voltage symphonious contortion is equivalent to 3.1%, the aggregate information current mutilation is 2.2% higher than the aggregate info voltage twisting. The pre-controller information current and voltage waveforms, working with V<sub>i</sub> = 220 V<sub>rms</sub> and without the third consonant bending diminishment method are exhibited in Fig. 21. Lessening the voltage contrast between the pinnacle of the info voltage and the yield voltage, the third symphonious bending increments, working with steady obligation cycle. The aggregate info current symphonious contortion is equivalent to 35.9% without the utilization of the third consonant diminishment method and the pre-controller power component is lessened to 0.951.

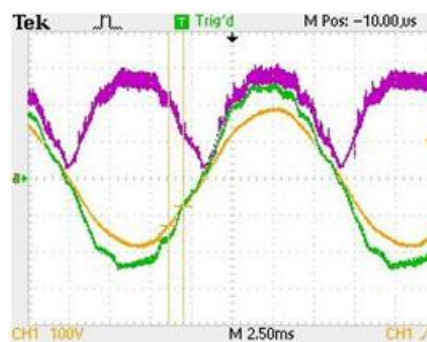


**Fig. 20. Input voltage and current operating with V<sub>i</sub>=127 V<sub>rms</sub> and with the third harmonic reduction technique (CH1 - Input voltage - 100 V/div, CH3 - L<sub>1</sub> current - 0.5 A/div, CH4 - Input current - 0.5 A/div).**



**Fig. 21. Input voltage and current operating with V<sub>i</sub>=220 V<sub>rms</sub> and without the third harmonic reduction technique (CH1 - Input voltage - 100**

V/div, CH3 -  $L_1$  current – 0.5 A/div, CH4 - Input current – 0.5 A/div).

The pre-regulator input current and voltage waveforms, operating with  $V_i = 220 V_{rms}$  and with the third harmonic distortion reduction technique are presented in Fig. 22.

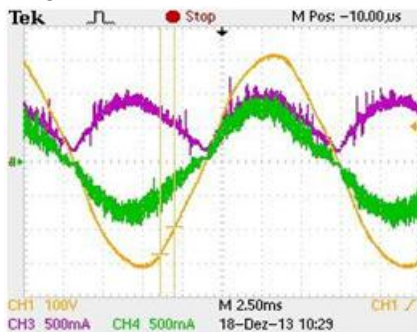


Fig. 22. Input voltage and current operating with  $V_i=220 V_{rms}$  and with the third harmonic reduction technique (CH1 - Input voltage - 100 V/div, CH3 -  $L_1$  current – 0.5 A/div, CH4 - Input current – 0.5 A/div).

The aggregate information current consonant bending is decreased from 35.9% to 8.84% with the use of the third symphonious diminishment procedure and the pre - controller power variable is expanded from 0.951 to 0.988. The aggregate info current bending is 5.74% higher than the aggregate information voltage mutilation. The pre-controller operation with ostensible yield power and information voltage equivalent to  $V_i=127 V_{rms}$  are exhibited from Fig. 23 to Fig. 30, considering the operation with the third consonant diminishment method. The  $L_1$  and  $L_2$  streams are exhibited in Fig. 23 and its present swell is near the hypothetical qualities 0.3 An and 3.56 An individually. The  $C_S$  and  $C_M$  capacitor voltages are displayed in Fig. 24. The hypothetical estimation of the  $C_S$  and  $C_M$  capacitor voltages at the pinnacle of the information voltage, considering the capacitor voltage swell invalid, is equivalent to 110 V and 290 V separately. The switch voltage and current are shown in Figs 25 and 26. The most compelling switch voltage is near 300V for an info voltage break even with 127  $V_{rms}$  and yield voltage equivalent to 400 V.

The streams in the diodes  $D_M$  and  $D_o$  are exhibited in Fig. 27. The hypothetical diode crest current is equivalent to 2 An and the hypothetical estimation of the diode conduction period is equivalent to  $t_d=17.45 \mu s$  at the pinnacle of the info voltage.

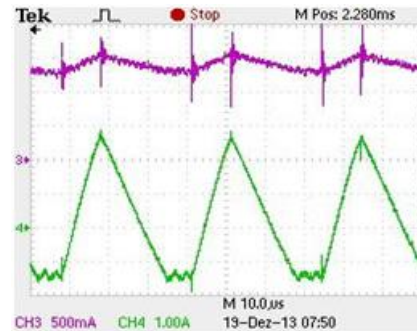


Fig. 23.  $L_1$  and  $L_2$  currents (CH3 –  $L_1$  current – 0.5 A/div, CH4 –  $L_2$  current – 1 A/div).

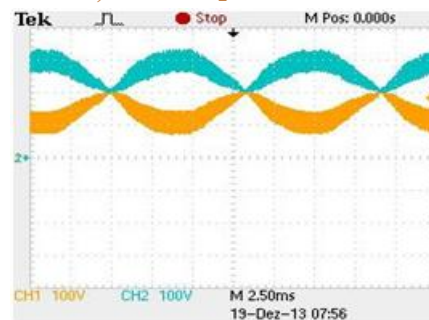


Fig. 24.  $C_S$  and  $C_M$  capacitor voltages (CH1 –  $C_S$  voltage - 100 V/div, CH2 –  $C_M$  voltage – 100 V/div).

The currents in the diodes  $D_M$  and  $D_o$  are presented in Fig. 27. The theoretical diode peak current is equal to 2 A and the theoretical value of the diode conduction period is equal to  $t_d=17.45 \mu s$  at the peak of the input voltage.

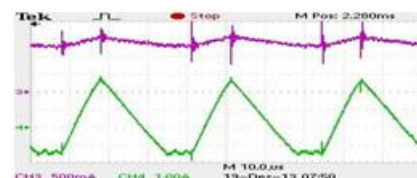


Fig. 23.  $L_1$  and  $L_2$  currents (CH3 –  $L_1$  current – 0.5 A/div, CH4 –  $L_2$  current – 1 A/div).

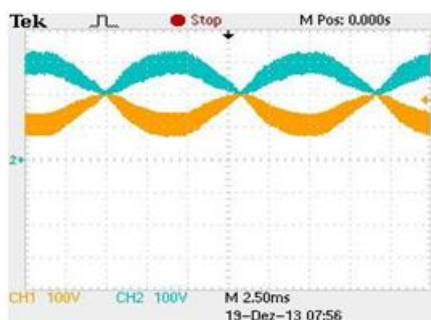


Fig. 24.  $C_S$  and  $C_M$  capacitor voltages (CH1 –  $C_S$  voltage - 100 V/div, CH2 –  $C_M$  voltage – 100 V/div).

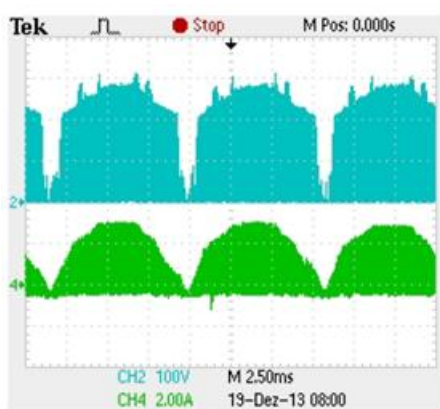


Fig. 25. Switch voltage and current (CH2 – Switch voltage - 100 V/div, CH4 – Switch current – 2 A/div, 2.5ms/div).

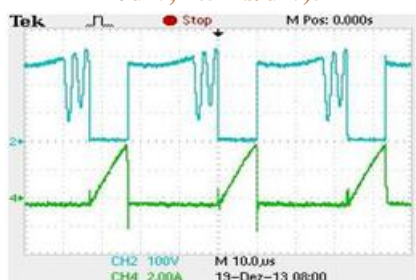


Fig. 26. Switch voltage and current (CH2 – Switch voltage - 100 V/div, CH4 – Switch current – 2 A/div, 10µs/div).

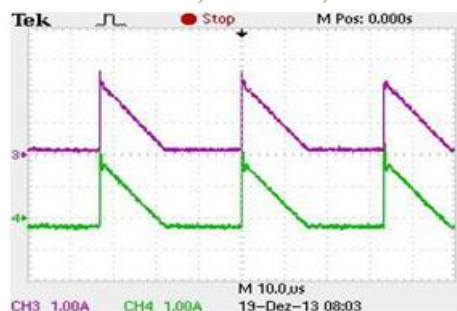


Fig. 27. Currents in the diodes  $D_M$  and  $D_O$  (CH3 –  $D_M$  current - 1 A/div, CH4 –  $D_O$  current – 1 A/div).

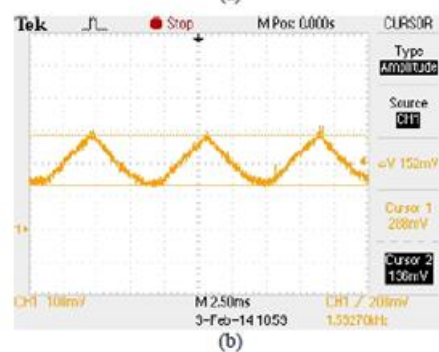
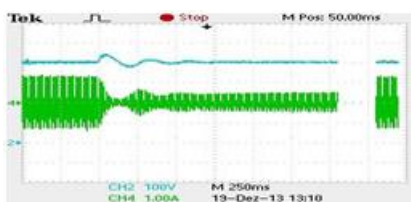


Fig. 28. PWM modulation signal (a)  $V_i=127$  V and (b)  $V_i=220$  V

The PWM modulation signal obtained from the product of the voltage control loop and the third harmonic reduction technique, as presented in Fig. 18, was applied to a digital to analog converter of the digital controller and is presented in Fig. 28 working with  $V_i=127$  Vrms and  $V_i=220$  Vrms. The voltage variety from 0 to 1 V compares to the obligation cyclevariation from 0 to 1. The adjustment signal got from the model is like the hypothetical result introduced in Fig.9. The dynamic reaction of the pre-controller is displayed in Figs. 29 and 30 for  $V_i = 127$  Vrms. Figure 29 demonstrates the dynamic reaction of the converter amid the heap change from 100% to 30% and Fig. 30 introduces the heap transient from 30% to 100%. The hypothetical effectiveness of the proposed converter working with a RMS information voltage meet 127 V has been evaluated considering the part parameters utilized as a part of the model appeared in Table IV.

Considering the RMS switch current ascertained by (58) and the  $R_{DSon}$  MOSFET with resistance square with  $240\ m\Omega$  (at  $80^\circ C$ ), the switch conduction misfortune is equivalent to  $0.22\ W$ . The normal current in the DM and Do diodes are equivalent to the yield current and considering the diode UF5408 (3A-800 V) utilized as a part of the model with a diode forward voltage equivalent to  $1.7\ V$ , the DM and Do diodes all out conduction misfortunes is equivalent to  $0.85\ W$ .



**Fig. 29. Load change from 100% to 30% (CH2 – Output voltage - 100 V/div, CH4 – Input current - 1 A/div, 250 ms/div).**

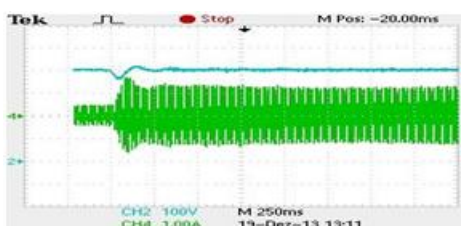


**Fig. 30. Load change from 30% to 100% (CH2 – Output voltage - 100 V/div, CH4 – Input current - 1 A/div, 250 ms/div).**

The normal current in the info span diodes is equivalent to  $0.37\ A$  and the aggregate conduction misfortunes of information diode scaffold is equivalent to  $2.52\ W$ . Consequently, the evaluated hypothetical proficiency of the proposed converter is equivalent to  $95.6\%$  considering the aggregate misfortunes of the inductors equivalent to  $1\ W$ . The established support converter presents comparative misfortunes in all parts. In any case, there is stand out diode in the converter yield, decreasing the diode conduction misfortunes in  $0.42\ W$  for the help model in contrast with the proposed converter model, bringing about a hypothetical productivity equivalent to  $96\%$ .

The same diode (UF5408) was utilized as a part of the trial models of the help and the changed SEPIC converters. Be that as it may, following the greatest voltage in the diodes DM and Do is dependably lower than the yield voltage ( $V_o=400V$ ), the diode UF5404 (3A-400V) with a diode forward voltage equivalent to  $1.0\ V$ , as exhibited in the diode producer inventory (Vishay), could be utilized as a part of the proposed converter prototype. Consequently, utilizing the diode 1N5408 as a part of the established help converter, the yield diode conduction misfortunes is equivalent to  $0.425\ W$  and utilizing the diode 1N5404 as a part of the proposed converter as the diodes DM and Do, the aggregate diode conduction misfortunes will be decreased from  $0.85\ W$  to  $0.5\ W$ . Likewise a lower  $R_{DSon}$  MOSFET could be utilized as a part of the proposed converter because of the lower switch voltage.

The exploratory proficiency of the proposed converter working with  $V_i=127\ V_{rms}$  and  $V_i=220\ V_{rms}$  are appeared in Figs. 31 and 32 separately, measured with the computerized power meter Yokogawa WT230. The model design was additionally changed to the traditional support rectifier displayed in Fig. 1 utilizing the same semiconductors of the proposed converter. The effectiveness bend of the help converter is exhibited considering an operation guide comparable toward the proposed converter utilizing an inductance equivalent to  $1.1\ mH$ . The productivity of the proposed converter working without output power equivalent to  $108\ W$  and  $V_i=127\ V_{rms}$  is equivalent to  $95.6\%$ , while for the support converter is equivalent to  $95.2\%$ .

The effectiveness of the proposed converter was measured likewise working with the third consonant diminishment method. The exploratory results demonstrate that not just a lessening of the third symphonious info current bending and the change of the rectifier power component happen, however there is additionally an augmentation in the converter effectiveness. The productivity increase utilizing the third consonant lessening regulation working with the ostensible yield is near  $0.5\%$  for the input voltage

$V_i=127 V_{rms}$  and equal to 1% for the input voltage  
 $V_i=220 V_{rms}$ .

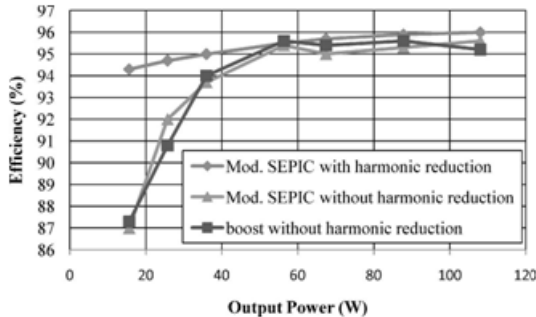


**Fig. 31. Pre-regulator efficiency for  $V_i=127 V_{rms}$ .**

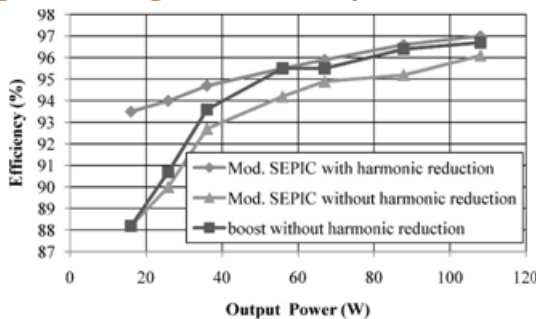


**Fig. 32. Pre-regulator efficiency for  $V_i=220 V_{rms}$ .**

In any case, a noteworthy proficiency increase happens in both info voltages for the light load operation, keeping up the converter effectiveness higher than 93% for all heap range. This operation trademark is fascinating for applications where the rectifier works amid a long stretch with low yield power.

**VIII. CONCLUSION:**

The hypothetical and trial investigation of the altered SEPIC converter utilized as pre-controller working as a part of DCM is displayed in this paper. The proposed converter exhibits low info current swell working in DCM and the switch and diodes voltages are lower than the yield voltage. The switch voltage decrease expands the converter unwavering quality and a lower RDSon MOSFET can be utilized relying upon the converter particular. The exploratory results gave working the third symphonious diminishment strategy demonstrates that the aggregate info current consonant twisting is decreased from 13% to 5.3% working with an information voltage meet 127 Vrms and is lessened from 35.9% to 8.84% working with an info voltage

equivalent to 220 Vrms, considering an aggregate information voltage symphonious contortion equivalent to 3.1%. The force element is higher than 0.988 with the third consonant decrease in all info voltage range. The proficiency working with information voltage equivalent to 127Vrms and yield power equivalent to 108 W is equivalent to 95.6%. The exploratory results demonstrate that there is likewise an addition in the converter productivity working with the third consonant diminishment regulation that basically happens at light load operation in 127 Vrms and 220 Vrms.

**REFERENCES:**

[1]O. García, J. A. Cobos, R. Prieto, P. Alou and J. Uceda, "Single Phase Power Factor Correction: A Survey", IEEE Transactions on Power Electronics, Vol. 18, No. 3, pp. 749-755, May 2003.  
 [2]M. M. Jovanovic and Y. Jang, "State-of-the-art, single-phase, active power-factor-correction techniques for high-power applications - An overview," IEEE Transaction on Industrial Electronics, Vol. 52, no. 3, pp. 701–708, June. 2005.  
 [3] D. S. L. Simonetti, J. Sebastian and J. Uceda, "The Discontinuous Conduction Mode Sepic and Cuk Power Factor Preregulators: Analysis and Design", IEEE Transactions on Industrial Electronics, vol. 44, no. 5, pp. 630 – 637, October 1997.  
 [4] M. Mahdavi and H. Farzanehfard, "Bridgeless SEPIC PFC Rectifier With Reduced Components and Conduction Losses", IEEE Transactions on Industrial Electronics, Vol. 58, No. 9, pp. 4153-4160, September 2011.  
 [5]A. A. Fardoun, E. H. Ismail, A.J. Sabzali and M. A. Al-Saffar, "New Efficient Bridgeless Cuk Rectifiers for PFC Applications", IEEE Transactions on Power Electronics, Vol. 27, No. 7, pp. 3292-3301, July 2012.  
 [6]E. H. Ismail, "Bridgeless SEPIC Rectifier with Unity Power Factor and Reduced Conduction Losses", IEEE Transactions on Industrial Electronics, Vol. 56, No. 4, pp. 1147- 1157, April 2009.  
 [7]B. Su, J. Zhang, and Z. Lu, "Totem-Pole Boost Bridgeless PFC Rectifier With Simple Zero-Current Detection and Full-Range ZVS Operating at the

Boundary of DCM/CCM," IEEE Transaction on Power Electronics , vol. 26, no. 2, pp.427-435, Feb. 2011.

[8] J. Zhang, B. Su and Z. Lu, "Single inductor three-level bridgeless boost power factor correction rectifier with nature voltage clamp," IET Power Electronics, vol. 5, no. 3, pp.358-365, March 2012.

[9] Y. Cho, and J.-S. Lai, "Digital Plug-In Repetitive Controller for Single-Phase Bridgeless PFC Converters," IEEE Transaction on Power Electronics, vol. 28, no. 1, pp.165-175, Jan. 2013.

[10] A. A. Fardoun, E. H. Ismail, A. J. Sabzali and M. A. Al-Saffar, "Bridgeless Resonant Pseudo Boost PFC Rectifier," IEEE Transaction on Power Electronics, vol. 29, no. 11, pp. 5949-5960, November 2014.

[11] R. Gules, W. M. Santos, F. A. Reis, E. F. R. Romaneli and A. A. Badin, "A Modified SEPIC Converter With High Static Gain for Renewable Applications", IEEE Transactions on Power Electronics, vol. 29, no. 11, pp. 5860-5871, November 2014.

[12] P. F. de Melo, R. Gules, E. F. R. Romaneli, R. C. Annunziato, "A Modified SEPIC Converter for High-Power-Factor Rectifier and Universal Input Voltage Applications", IEEE Transaction on Power Electronics, vol. 25, no. 2, pp. 310-321, Feb. 2010.

[13] J. Lazar and S. Cuk, "Open Loop Control of a Unity Power Factor, Discontinuous Conduction Mode Boost Rectifier", International Telecommunications Energy Conference - INTELEC '95, pp. 671 – 677, 1995.

[14] D. S. L. Simonetti, J. Sebastain and J. Uceda, "A Small Signal Model For Sepic, Cuk And Flyback Converters As Power Factor Preregulators In Discontinuous Conduction Mode", IEEE Power Electronics Specialists Conference - PESC '93, pp. 735 – 741, 1993.

[15] R. W. Erickson , D. Maksimovic, "Fundamentals of Power Electronics Second Edition", Kluwer Academic Publishers, New York, January 2001.

[16] V. Vorperian, "Simplified analysis of PWM converters using model of PWM switch. II.

Discontinuous conduction mode," IEEE Transactions on Aerospace and Electronic Systems, vol.26, no.3, pp.497- 505, May 1990.